

# Surface-sensitive *K*-edge absorption spectroscopy on clean and hydrogen-terminated diamond (111) and (100) surfaces

R. Graupner, J. Ristein, and L. Ley

*Institut für Technische Physik, Universität Erlangen, Erwin-Rommelstr. 1, 91058 Erlangen, Germany*

Ch. Jung

*BESSY GmbH, Lentzeallee 100, 14195 Berlin, Germany*

(Received 2 December 1998; revised manuscript received 9 July 1999)

We present a detailed electron yield spectroscopy study of the pre-*K*-edge features of single-crystal diamond (100) and (111) surfaces which are induced by optical transitions from the C  $1s$  core level into excited states. Both hydrogen-terminated and hydrogen-free surfaces were investigated. A sharp maximum at  $\hbar\omega = 287.2$  eV in the spectra of the (111) and (100) surfaces is characteristic of the monohydrogenated surfaces, which is interpreted as a strongly localized intramolecular excitation within the C-H bond of a surface atom. The clean diamond surfaces show maxima in the absorption spectra at  $\hbar\omega = 284.6$  eV for the (111) surface, and at 284.15 and 286.3 eV for the (100) surface which are interpreted as surface core excitons. From the polarization dependence of the intensities of these features and by using dipole selection rules, the point-group symmetry of the excited states involved in the optical transition is deduced. The transition energies of the absorption maxima of the clean surface are discussed in terms of pertinent band-structure calculations and excitonic effects. [S0163-1829(99)14247-4]

## I. INTRODUCTION

The possibility to deposit diamond from the gas phase in the form of thin films by chemical vapor deposition has stimulated attempts to utilize diamond as a material for electronic devices. Due to the lack of an electrically active donor, electronic devices have to work as unipolar devices (e.g., Schottky diodes, field-effect transistors) based on undoped or *p*-type diamond.<sup>1,2</sup> These devices rely on the properties of the interface between the semiconductor and the metal or insulator. Some of the properties of the clean or hydrogen-terminated surfaces are believed to be maintained even after a metallization, such as the dipole layer induced by a hydrogen termination of the surface,<sup>3</sup> and therefore control the interface properties to a large extent. Whereas occupied surface states of diamond (100) and (111) have been investigated extensively by photoemission,<sup>4</sup> hardly any experimental information is available on unoccupied surface states. This issue is the target of the present paper.

As an experimental method we use *K*-edge absorption spectroscopy. This method is widely used for the determination of  $sp^2/sp^3$  ratios in carbon-based materials.<sup>5-7</sup> The reason is that the presence of  $\pi$  bonding which is characteristic of  $sp^2$  hybridized carbon can easily be identified by the C  $1s \rightarrow \pi^*$  transition which is lower in energy than the C  $1s \rightarrow \sigma^*$  transition observed as absorption threshold in  $sp^3$ -coordinated material. Similarly, any  $\pi$  bonds which occur as a result of reconstruction of the surface on the otherwise purely  $\sigma$ -bonded diamond are expected to show up in the *K*-edge absorption spectra on the hydrogen-free surface. By the same token, unoccupied C-H antibonding states can possibly show up, provided they lie in the fundamental gap of diamond.

## II. EXPERIMENT

The samples we investigated are type-IIb single-crystal diamonds (semiconducting due to boron acceptors). The (100) surface was prepared by mechanical polishing, while the (111) surface was a cleavage plane. Prior to measurement the samples were exposed *ex situ* to a microwave-excited hydrogen plasma at substrate temperatures of 800–900 °C. This plasma polishing process is known to result in atomically flat, hydrogen terminated surfaces.<sup>8,9</sup> The (100) surface exhibits a  $2 \times 1$  LEED (low-energy electron-diffraction) pattern which is characteristic for a surface terminated by one hydrogen atom per surface atom<sup>10</sup> (monohydride dimer-row reconstruction), whereas the (111) surface exhibits a  $1 \times 1$  LEED pattern due to a bulklike termination of the surface with hydrogen. However, in a recent study we reported that additional hydrocarbons are adsorbed on the surfaces after the plasma preparation process.<sup>11</sup> These hydrocarbons desorb upon annealing in UHV at temperatures below the temperature necessary to desorb the hydrogen passivation. Annealing the surfaces further, i.e., above the hydrogen desorption temperature, leads in both cases to clean,  $2 \times 1$ -reconstructed surfaces that exhibit the intrinsic surface states that we demonstrated elsewhere.<sup>4</sup> We note that all annealing temperatures given in this paper were measured using an optical pyrometer. As diamond is transparent for the wavelength used by the pyrometer, the temperatures given are those of the Ta sample holder. Identifying this temperature reading with the surface of the diamond causes an uncertainty which we estimate to about  $\pm 100$  °C from experience gained in the preceding experiments. For a true temperature measurement of the diamond samples, more elaborate methods have to be used.<sup>12</sup>

All spectra were recorded using the plane grating monochromator PM-5 (Petersen monochromator) at the BESSY I

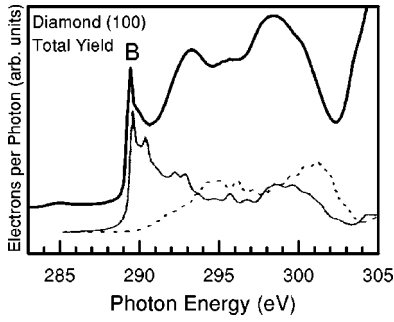


FIG. 1.  $K$ -edge absorption spectrum (total yield) of a diamond (100) surface (upper curve).  $B$ : bulk core exciton of diamond. Lower curves: calculated  $K$ -edge absorption spectra by Shirley with (full line) and without (dashed line) core-hole effects.

storage ring in Berlin. The typical resolution of the light source is 0.1 eV at  $\hbar\omega=300$  eV (the exit slit width is 100  $\mu\text{m}$ ). All spectra are corrected for variations of the beam current in the storage ring as well as for the spectral transmission of the beamline by recording the photon flux using a calibrated  $\text{Ga}_x\text{As}_{1-x}\text{P}$  photodiode. The exact photon energy was determined by measuring the difference in kinetic energies of the photoelectrons of the Ta  $4f$  core level of the sample holder excited by the first- and second-order diffracted light of the grating monochromator.

The  $K$ -edge absorption spectra were measured in the yield mode, i.e., by monitoring the electron flux emitted by the sample as a result of secondary processes which fill the  $K$ -shell ( $1s$ ) hole following the primary absorption process. The electron yield is thus proportional to the absorption coefficient.<sup>13</sup>

We measured the  $K$ -edge absorption spectra in the total yield mode, collecting all secondary electrons emitted from the surface as well as in the partial yield mode, which is restricted to electrons with minimum escape depth (0.5–1 nm) and therefore provides a very high surface sensitivity. The comparison between total and partial yields therefore readily identifies surface-related features. Another way to separate bulk from surface absorption is achieved by using the polarization dependence of the optical transitions. Dipole transitions between bulk states of diamond do not depend on the polarization direction of the light on account

of the cubic symmetry of the lattice. This, however, does not hold for surface absorption, where the symmetry normal to the surface is broken. Therefore, spectra were taken with normal incidence of the light ( $\Theta_{\text{incid}}=0^\circ$ ) so that the electric-field vector had no component normal to the sample surface. We also used an incidence angle of  $\Theta_{\text{incid}}=60^\circ$ , where the electric field vector of the linearly polarized synchrotron radiation forms an angle of  $60^\circ$  with respect to the sample surface ( $p$  polarization). The angle between the incoming light and the electron detector is fixed at  $60^\circ$ .

### III. RESULTS

The  $K$ -edge absorption spectrum of a diamond (100) surface (total yield) is shown in Fig. 1, upper curve. The sharp feature at  $\hbar\omega=289.43$  eV ( $B$ ) is caused by the creation of the bulk core exciton of diamond—i.e., an electron in the conduction band bound to a core hole—and it marks the onset of the bulk absorption. The importance of core-hole effects was pointed out by recent *ab initio* calculations by Shirley,<sup>14</sup> which are shown as the lower two curves in Fig. 1. The calculated spectra are adjusted in energy to the measured spectrum so that the core-exciton peaks coincide. The full line is the calculated absorption spectrum including core-hole interaction, the dashed line that without core-hole effects.<sup>14</sup> The inclusion of electron-hole interactions reproduces most of the spectral features of the measured spectrum, whereas the exclusion of core-hole effects completely fails to explain the experimental data. The dip in the yield spectrum at  $\hbar\omega=302.5$  eV is caused by an absolute energy gap in the conduction-band structure of diamond.<sup>15</sup> In this paper we will concentrate on the pre-edge features, seen as weak structures below  $\hbar\omega\approx 289$  eV. These structures are (at least partly) induced by transitions into unoccupied surface states and their position and intensities are gathered in Tables I and II.

In the upper spectra of Figs. 2(a) and 2(b), partial electron yield spectra of the diamond (111) and (100) surfaces in the as prepared state after plasma hydrogenation are compared. For the (111) surface [Fig. 2(a)] the total yield spectrum for  $\vartheta_{\text{incid}}=60^\circ$  is also shown to illustrate that the pre-edge features in the spectra ( $\hbar\omega<289$  eV) are related to the surface. Both the (100) and (111) surfaces show very similar spectra.

TABLE I. Energies, linewidths (in eV), and absorption strengths of characteristic features in the subthreshold  $C 1s$  yield spectra of the diamond (111) surface.  $T_A$  is the annealing temperature, and  $\Theta_{\text{inc}}$  refers to the light incidence angle.

Surface preparation	LEED pattern	Absorption maximum	$\hbar\omega$ (FWHM)	Intensity at		Origin
				$\Theta_{\text{inc}}=60^\circ$	$\Theta_{\text{inc}}=0^\circ$	
as prepared	$1\times 1$	broad maximum <sup>a</sup>	285.0	weak	strong	nondiamond defect states
H-terminated + hydrocarbon contamination		$S_A$	287.8 (1.1)	strong	absent	antibonding C-H states (hydrocarb.)
$T_A=600^\circ\text{C}$ monohydrogenated	$1\times 1$	$S_H$	287.3 (0.60)	strong	absent	antibonding C-H monohydride states
$T_A=1200^\circ\text{C}$ hydrogen free	$2\times 1$	$S$	284.6 (0.50)	strong	absent	surface core exciton

<sup>a</sup>The broad maximum is present for all surface preparations.

TABLE II. As in Table I for the (100) surface.

Surface preparation	LEED pattern	Absorption maximum	$\hbar\omega$ (FWHM)	Intensity at		Origin
				$\Theta_{\text{inc}}=60^\circ$	$\Theta_{\text{inc}}=0^\circ$	
as prepared	$2\times 1$	broad maximum <sup>a</sup>	285.0	weak	strong	nondiamond defect states
H-terminated + hydrocarbon contamination		$S_A$	287.8 (1.0)	strong	absent	antibonding C-H states (hydrocarb.)
$T_A=400^\circ\text{C}$ monohydrogenated	$2\times 1$	$S_H$	287.3 (0.60)	weak	absent	antibonding C-H monohydride states
$T_A=1200^\circ\text{C}$ hydrogen free	$2\times 1$	$S_{\Gamma_1}$	284.15 (0.57)	very strong	absent	surface core exciton ( $\Gamma_1$ symm.)
		$S_{\Gamma_3,\Gamma_4}$	286.3 (0.50)	absent	strong	surf. core exc. ( $\Gamma_3$ or $\Gamma_4$ symm.)

<sup>a</sup>The broad maximum is present for all surface preparations.

At  $\hbar\omega=289.5$  eV we detect a broad maximum which is seen in all yield spectra of diamond irrespective of surface preparation. The fact that the intensity of this broad maximum is higher when normal light incidence ( $\Theta_{\text{incid}}=0^\circ$ ) is used [the lower curve of Fig. 2(a)] reflects the surface origin of these features. For normal light incidence, electrons are

detected at an angle of  $\vartheta_{\text{em}}=60^\circ$  with respect to the surface normal, and hence the effective escape depth is only half of the escape depth at  $\Theta_{\text{incid}}=60^\circ$ , where  $\vartheta_{\text{em}}=0^\circ$ . The inset of Fig. 2(b) illustrates the two geometries. Besides the broad maximum around 285 eV, a second peak  $S_A$  with a full width at half maximum (FWHM) of about 1 eV is located at 287.8 eV. This peak, in contrast to the broad maximum at 285 eV, is not enhanced when going from  $\Theta_{\text{incid}}=60^\circ$  ( $\vartheta_{\text{em}}=0^\circ$ ) to  $\Theta_{\text{incid}}=0^\circ$  ( $\vartheta_{\text{em}}=60^\circ$ ), but is strongly reduced.

As already mentioned, the surfaces prepared in a hydrogen plasma are found to be partially terminated by hydrocarbons.<sup>11</sup> These hydrocarbons desorb at an annealing temperature of around  $400^\circ\text{C}$ , which results in a change in the yield spectra (Fig. 3). While the partial yield spectrum at  $\Theta_{\text{incid}}=0^\circ$  remains virtually unchanged, the feature  $S_A$  centered at 287.8 eV (Fig. 2) is replaced by a narrower peak (a FWHM of 0.60 eV) at  $\hbar\omega=287.3$  eV in the  $\Theta_{\text{incid}}=60^\circ$  spectrum after annealing ( $S_H$  in Fig. 3). This feature occurs at exactly the same photon energy and has identical line shapes on both surfaces, albeit twice as intense on (111) as on (100). In the case of (111) the LEED pattern still shows sharp  $1\times 1$ -spots of a bulklike termination, indicating that the surface is still hydrogenated. From the similarity of the spectra we draw the same conclusion for the (100) surface.

Annealing the (111) surface above  $1000^\circ\text{C}$  finally leads to hydrogen desorption, and produces the spectra of the clean surfaces. The  $S_H$  feature of the monohydrogenated surfaces is absent, and now characteristic differences occur between the spectra of diamond (100) and (111) (Fig. 4). For (111) a peak at  $\hbar\omega=284.6$  eV ( $S$ ) appears which is only visible for  $\Theta_{\text{incid}}=60^\circ$  [Fig. 4(a)]. The hydrogen-free,  $(2\times 1)$ -reconstructed diamond (100) surface [Fig. 4(b)], however, exhibits a peak at  $\hbar\omega=286.3$  eV ( $S_{\Gamma_3,\Gamma_4}$ ) under normal light incidence, whereas an intense maximum at 284.15 eV ( $S_{\Gamma_1}$ ) is observed using  $\Theta_{\text{incid}}=60^\circ$ . All three resonances observed on the clean diamond surfaces are notably sharper (the FWHM is  $0.5 \dots 0.57$  eV) than the peak  $S_A$  of the hydrocarbon adsorbates (the FWHM is  $1.0 \dots 1.1$  eV) and even slightly sharper than the monohy-

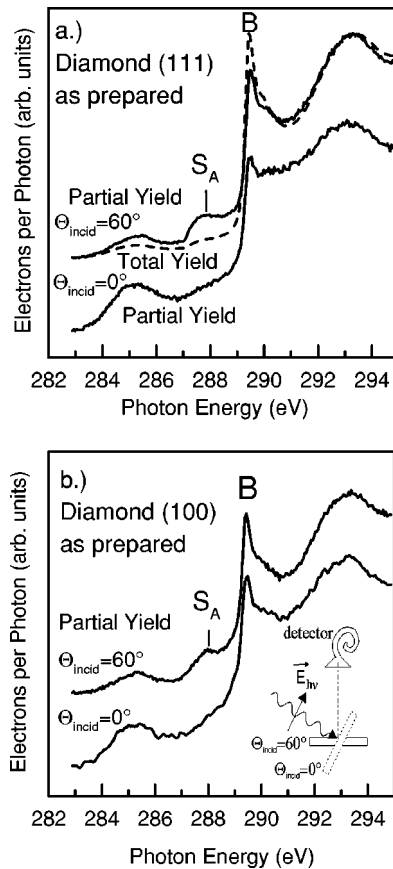


FIG. 2. Yield spectra of (a) a diamond (111) and (b) a diamond (100) surface after preparation in a microwave hydrogen plasma, recorded with different incidence angle of the excitation light. The inset in (b) illustrates relative positions and orientations of the incoming light, the sample surface, and the electron detector.

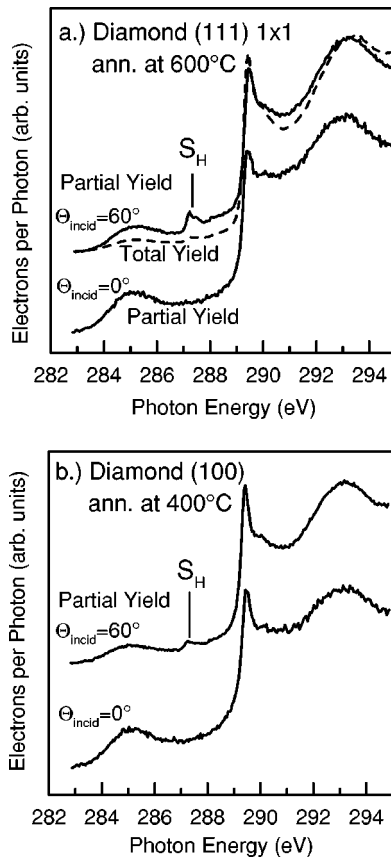


FIG. 3. Yield spectra of (a) a diamond (111) surface annealed at 600 °C and (b) a diamond (100) surface annealed at 400 °C. Both surfaces have retained a hydrogen passivation after these annealing steps.

drude peak  $S_H$  (the FWHM is 0.6 eV). (The origin of the notations  $S_{\Gamma_1}$  and  $S_{\Gamma_3-\Gamma_4}$  will be explained below.)

#### IV. DISCUSSION

##### A. As-prepared surfaces

The pre-edge absorption spectra of the as-prepared diamond (100) and (111) surfaces (Fig. 2) both show two rather broad absorption maxima at  $\hbar\omega=285$  and at 287.9 eV ( $S_A$ ). The maximum around  $\hbar\omega=285$  eV appears in all spectra of the hydrogen-terminated surfaces as well as in those of the annealed surfaces. The energy of this structure resembles a broadened C  $1s \rightarrow \pi^*$  transition which is seen in graphite as well as in all unsaturated hydrocarbon molecules, also centered at 285 eV.<sup>5,16</sup> We therefore attribute this maximum to transitions into empty defect states that are not intrinsic to the diamond surfaces. The peak  $S_A$  is within the uncertainty of our experiment situated at the same photon energy (287.8 eV) on diamond (100) and (111), and vanishes after moderate annealing. We therefore assign this peak to hydrocarbon adsorbates which are easily thermally desorbed. This interpretation is supported by the fact that an absorption resonance around  $287.5 \pm 0.3$  eV is found as the dominant feature below the C  $1s$  ionization threshold in a large variety of saturated hydrocarbon molecules.<sup>17-19</sup>

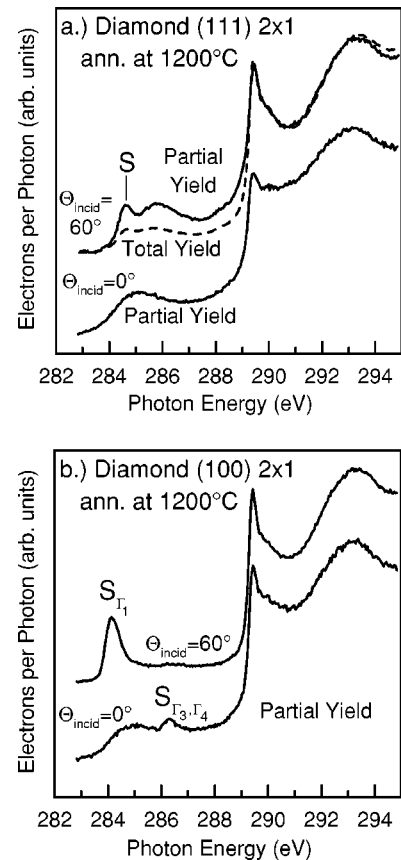


FIG. 4. Yield spectra of (a) a clean, ( $2 \times 1$ )-reconstructed diamond (111) surface and (b) a clean, ( $2 \times 1$ )-reconstructed diamond (100) surface, both obtained after annealing at 1200 °C.

##### B. H-terminated surfaces

For both surfaces the first annealing step [400 and 600 °C for (100) and (111), respectively] results in a desorption of the hydrocarbons and yields the monohydrogenated diamond surfaces. The peaks at  $\hbar\omega=287.2$  eV ( $S_H$ ) are characteristic for these surfaces (Fig. 3). Morar *et al.*<sup>20</sup> also performed  $K$ -edge absorption spectroscopy on hydrogen-terminated diamond (111). They found two peaks at  $\hbar\omega=284.7$  and 287.3 eV. The peak at 284.7 eV resembles our graphitic peak at 285 eV which is not intrinsic to the diamond surfaces. Their peak at 287.3 eV has a full width at half maximum of 1.6 eV and is thus much broader than our structure  $S_H$  (the FWHM is 0.6 eV). It might be a superposition of the  $C-H^*$  adsorbate resonances and the monohydride signal  $S_H$  at 287.2 eV. The differences in the spectra measured here and those of Morar *et al.* are caused by different sample preparation techniques. Morar *et al.* prepared their sample by cleavage under hydrogen atmosphere. As no source for atomic hydrogen was present, this procedure might not lead to a surface which is completely hydrogen terminated.

The interpretation of  $S_H$  can be approached from two different perspectives. The final (two-particle) state which gives rise to a resonance in the absorption cross section involves a strongly localized C  $1s$  core hole carrying a positive charge and an electron in a less localized but jet bound state which “feels” the positive charge of the core hole as well as the specific periodic potential of the surface. In general, both interactions have to be taken into account simultaneously.



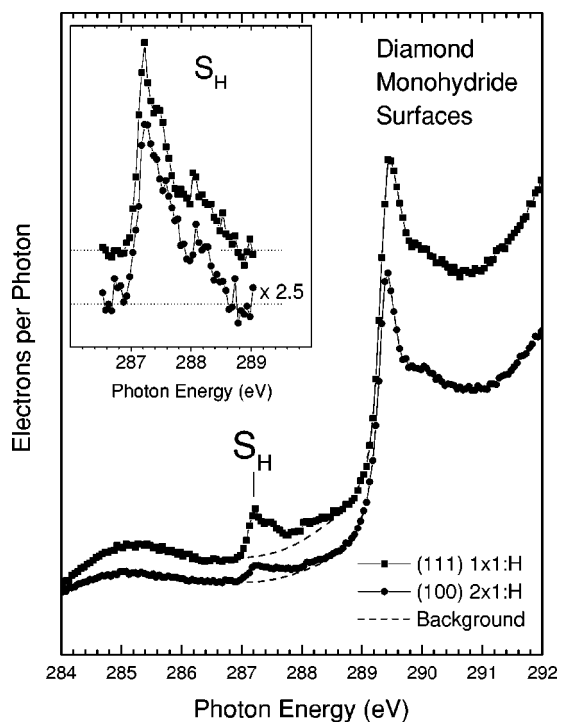


FIG. 5. Line-shape analysis of the  $S_H$  absorption resonance on the monohydrogenated (100) and (111) surface demonstrating the identical signature.

From the perspective of solid-state surface physics this is done by using the characteristic surface-state band of a specific surface as a basis set for the electron part of the final-state wave function. The Coulomb interaction between electron and core hole is then treated as a second-order perturbation, with the result that the final (bound) state of the optical transition is interpreted as a surface core exciton. It has a specific binding energy with respect to the continuum (i.e., the unbound final states), and a wave function which is strongly influenced by the periodic potential of the solid. This surface physics approach thus appears to be appropriate when the specific signature of the surface is reflected in the  $K$ -edge absorption spectrum, as is the case for the clean diamond (100) and (111) surfaces.

A different approach is usually taken in molecular physics. The electron's interaction with the charge of the core hole is in this case considered as the dominant effect, and the excited state probed by near-edge x-ray-absorption fine-structure spectroscopy and electron-energy-loss experiments is interpreted in terms of an excited molecular or even atomic state. The interaction of the electron with the periodic potential of the surface is in this case neglected. The molecular approach is expected to be the appropriate one for physisorbed adsorbates, i.e., those bound only weakly to the surface by van der Waals forces. It is remarkable that peak  $S_H$  observed on the monohydrogenated diamond (100) and (111) surfaces seems to fulfill these criteria. Its line shape is identical on both surfaces as illustrated in Fig. 5, and the peak energy of 287.3 eV, moreover, falls into the range where resonances of saturated hydrocarbons such as cycloalkanes (287...287.7 eV)<sup>19</sup> and alkanes (287...288 eV)<sup>17</sup> occur. Although it appears to be still a matter of debate to what extent the final states participating in these hydrocarbon

resonances have molecular C-H\* or atomic, i.e., Rydberg state character, the local nature of the excitation is unambiguous. From its similarity with the hydrocarbon resonances we conclude therefore that the  $S_H$  peak of the monohydrogenated diamond surfaces represents a strongly localized transition. The electron-hole interaction is obviously much stronger than the interaction between the ordered array of C-H units which give rise to the dispersion of the surface state band, as it is calculated theoretically within the local-density approximation. This band indeed has a very similar width and position for diamond (100)2×1:H (Ref. 21) and (111) 1×1:H.<sup>22</sup> Nevertheless, the evidence for the local molecular character of the resonance opposes its interpretation as a surface core exciton in the language of solid-state physics.

### C. Clean (100) and (111) surfaces

The situation is different for the clean diamond surfaces (Fig. 4). Here the resonances  $S$  on diamond (111) (2×1) and  $S_{\Gamma_1}$  and  $S_{\Gamma_3, \Gamma_4}$  on diamond (100) (2×1) depend clearly on the nature of the surface. An interpretation as surface core excitons involving the respective surface states is more appropriate here. In the majority of calculations for the surface states, electron-hole interaction is neglected, and in the UV excited photoemission and optical absorption experiments from which band-structure energies are usually inferred electron-hole interaction is negligible on our energy scale. As explained above, this is markedly different in the yield experiment, where a strongly localized hole state is involved. From the comparison between measured and calculated x-ray absorption spectra in Fig. 1, it is evident that core-hole interaction plays an important role. Therefore the question arises where the conduction-band minimum (CBM) has to be placed. As the bulk core exciton ( $B$ ) is the dominating structure, the knowledge of the core-exciton binding energy  $\Delta E_{ex} = E_{CBM} - E(B)$  would fix  $E_{CBM}$ . However, there is an ongoing debate on the binding energy of the core exciton in diamond.<sup>15,23-25</sup> Morar *et al.*,<sup>15</sup> for example, obtained an exciton binding energy of  $\Delta E_{ex} = 0.19$  eV by fitting the measured absorption spectra to the theory of Elliott,<sup>26</sup> which, however, is only valid for loosely bound, hydrogenlike Wannier excitons. We note that a fit of our measurements using this theory does not lead to a satisfactory result, neither using the parameters of Morar *et al.* nor any other set of parameters. Meanwhile, there appears to be a general consensus that  $\Delta E_{ex}$  as determined by Morar *et al.* is too low and that vibrational effects, i.e., a local relaxation of the lattice, have to be taken into account in addition to the Coulomb interaction between the electron and hole.<sup>25,27-29</sup> Nevertheless, some interesting conclusions can be drawn from our results if we place them in a one-electron scheme as is done in Fig. 6. We use the core exciton  $B$  as our fiducial point. Following our discussion of the core-exciton binding energy, we shifted the one-particle energies on the left-hand side by  $\Delta E_{ex} = 0.25$  eV as calculated for the allowed optical transition by Mauri and Car<sup>28</sup> with respect to our  $K$ -edge absorption data on the right-hand side. Note that this value is smaller than the exciton ground-state binding energy when lattice relaxation plays a significant role.<sup>28</sup> The left-hand axis is thus a one-particle energy scale with  $E_{CBM}$  as zero.

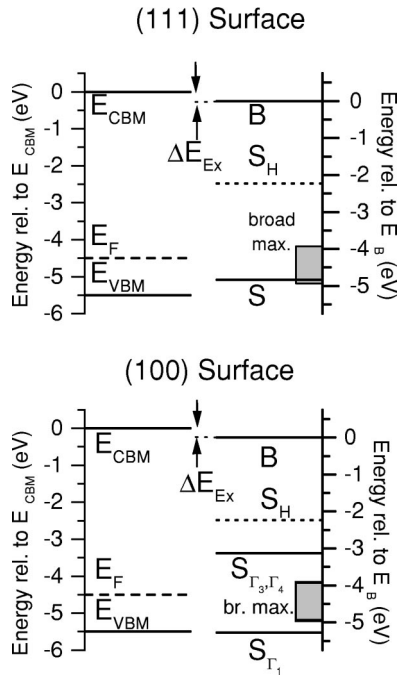


FIG. 6. Schematic energy diagram comparing the one-particle energies  $E_{CBM}$ ,  $E_{VBM}$ , and  $E_F$  with the resonances in the  $K$ -edge absorption spectra for the (111) (upper panel) and the (100) surface (lower panel). The bulk core exciton at a photon energy of 289.5 eV was used as a common reference in all spectra. For this diagram, its binding energy  $\Delta E_{ex}$  was set to 0.25 eV as calculated by Mauri and Car. The position of  $E_F$  applies to the hydrogen-free surfaces.

The position of the Fermi level with respect to  $E_{VBM}$  (VBM is the valence-band maximum) has been determined using valence-band photoemission. On the hydrogen-free diamond (100) and (111) surfaces, values of 0.8–1.4 eV for  $E_F - E_{VBM}$  have been measured.<sup>4,30,31</sup> The average position of  $E_F$  is thus marked 1.0 eV above  $E_{VBM}$  in Fig. 6.

On clean diamond (100) a band of unoccupied surface states is predicted theoretically which extends from the CBM down into the band gap. The band minimum lies 1.3 eV above the VBM, and the highest occupied surface state lies below the VBM. If we use the minimum as a reference,  $S_{\Gamma_1}$  corresponds to an exciton with a binding energy of 1.3 eV (see Fig. 6). The second resonance,  $S_{\Gamma_3, \Gamma_4}$  is degenerate with the empty surface-state band, and must therefore be interpreted as an excitonic resonance.

The (111) surface is predicted to be metallic with surface states extending throughout the gap.<sup>22</sup> In light of these calculations peak  $S$  found on diamond (111) has to be interpreted as an excitonic resonance as well. We should mention, however, that recent angle-resolved photoemission spectra of that surface showed a gap on the clean, reconstructed diamond (111) surface.<sup>4</sup> It extends from 0.5 eV to at least 1.0 eV above the VBM. The surface core exciton  $S$  in Fig. 6 is placed at 0.35 eV above the VBM, and thus coincides with the lower edge of the experimentally determined surface gap.

In III-V semiconductors, binding energies of 0.3–1.5 eV have been measured for surface core excitons.<sup>32</sup> These large binding energies are the result of the two-dimensional nature

of the surface excitons and the reduced screening at the surface. Since the dielectric constant of diamond ( $\epsilon=5.7$ ) is small compared to III-V compounds, an exciton binding energy of  $S_{\Gamma_1}$  on the diamond (100) surface at the upper end of this scale comes as no surprise.

The level scheme of Fig. 6 is drawn under the additional assumption that the energy of the initial state for the transitions  $C 1s \rightarrow B$  and  $C 1s \rightarrow S_{\Gamma_1}$  is the same. In the core-level spectra of clean (hydrogen-free) diamond surfaces, a  $C 1s$  surface component is observed which is shifted by 0.9 eV toward lower binding energy [1.0 eV on the (111)-surface].<sup>11</sup> If this component is taken as the initial state for the surface core excitons, and the bulk component is assumed for the bulk core level exciton, the positions of  $E_F$  and  $E_{VBM}$  in Fig. 6 are also lower by 0.9 and 1.0 eV, respectively, as discussed by Morar *et al.*<sup>20</sup> This, however, only holds true if the surface core-level shift observed in photoemission is an *initial-state effect*. We rather believe that this component in the  $C 1s$  photoelectron spectra is induced by a different relaxation of the remaining  $(N-1)$ -electron system upon formation of a photohole in a surface atom compared to a hole in a bulk atom (*final-state effect*).<sup>11</sup>

#### D. Symmetry of core-level excitations

The use of the dipole selection rule for optical transitions allows us to identify the point-group symmetry of the final states. To this end we consider the matrix element of the dipole operator for the electron transition between the  $C 1s$  core state and its excitonic wave function. In our experiment we employed two different polarizations of the excitation light. Normal incidence with no component of the dipole operator perpendicular to the sample surface ( $\Theta_{incid}=0^\circ, p_z=0$ ) and  $\Theta_{incid}=60^\circ$ , for which the in-plane component *and* the normal component of the dipole operator is finite ( $p_{\parallel} \neq 0, p_z \neq 0$ ). In changing the incidence angle of the light the azimuthal direction of the in-plane component of the dipole operator  $p_{\parallel}$  was not changed. The surface-related features  $S_A$  and  $S_H$  on both hydrogenated (100) and (111) surfaces as well as  $S$  of the clean (111):(2 $\times$ 1) and  $S_{\Gamma_1}$  for the clean (100):(2 $\times$ 1) all appear for grazing incidence ( $\Theta_{incid}=60^\circ$ ) and *are absent for normal incidence*. Thus, for these features the transition at  $\Theta_{incid}=60^\circ$  has to be induced by the normal component of the dipole operator  $p_z$ . As the  $C 1s$  core level is transformed under all symmetry operations of the point group of the surface corresponding to the totally symmetric representation ( $\Gamma_1$ ),  $p_z$  (which transforms as  $\Gamma_1$  as well) can only induce optical transitions into final states of  $\Gamma_1$  symmetry as well.

A different polarization dependence is observed for  $S_{\Gamma_3, \Gamma_4}$  at  $\hbar\omega=286.3$  eV on the clean (100):(2 $\times$ 1) surface. Here the transition has to be induced by the parallel component of the dipole operator  $p_{\parallel}$ , and the final-state transforms according to the  $\Gamma_3$  or  $\Gamma_4$  representations of the point group of the (100):(2 $\times$ 1) surface ( $C_{2v}$  or  $2mm$ ). This means that the wave function is symmetric with respect to the mirror planes, and changes sign upon rotation by 180 $^\circ$ .

If one were able to prepare a surface reconstructed in one single domain, one should be able to distinguish between these two irreducible representations by investigating how

the intensity depends on the azimuthal orientation of the electric-field vector. On our samples, however, this is not possible as a mixture of two domains, rotated by  $90^\circ$ , was always present with equal weight.

## V. CONCLUSION

We have identified optical transitions from the C  $1s$  core level into excited states on clean and hydrogen-terminated diamond (100) and (111) surfaces utilizing the pre- $K$ -edge resonances of the absorption spectrum. On the as-hydrogenated surfaces, resonances occur at around 287.8 eV with no specific signature characteristic for the surfaces. They are attributed to molecular excitations within hydrocarbon adsorbates. Mild annealing removes these adsorbates, but retain a hydrogen passivation. On these monohydrogenated surfaces absorption resonances occur at a similar photon energy [as for the adsorbates ( $\hbar\omega=287.3$  eV)], but are notably sharper and significantly shifted. Their energy and line shape are, however, not specific for the respective surface, and thus we associate them with strongly localized excitations within the monohydride units of the surface atoms. Their spectroscopic signature is dominated by the electron's interaction with the core hole rather than with the periodic potential of the surface. The situation is different for the clean, reconstructed surfaces. Here again, sharp resonances occur which are now clearly different for diamond (100)

( $\hbar\omega=284.15$  eV and  $\hbar\omega=286.3$  eV) and (111) (284.6 eV). Moreover, their polarization dependence follows specific selection rules which allows a determination of the symmetry of the excited states. Consequently they are interpreted as surface core excitons or excitonic resonances. However, their energetic positions are not linked consistently to surface-state bands as would be expected for delocalized Wannier-type surface core excitons. Also, in the case of the clean surfaces we therefore interpret the pre- $K$ -edge absorption resonances as rather localized Frenkel-type surface core excitons, again confirming the strong electron-hole interaction. The latter may be due to the lack of electrostatic screening by the valence electrons of diamond, and thus linked to the low dielectric constant of the material.

## ACKNOWLEDGMENTS

We would like to thank K. Janischowsky and R. Stöckel for the hydrogen plasma preparation of our samples. The authors gratefully acknowledge financial support by the Deutsche Forschungsgemeinschaft (Project No. Le 643/5-3) carried out under the auspices of the trinational "D-A-CH" cooperation of Germany, Austria, and Switzerland on the "Synthesis of Superhard Materials." The measurements at BESSY were supported by the Bundesminister für Bildung, Wissenschaft, Forschung und Technologie under Contract No. 05 622 WEA 7.

- 
- <sup>1</sup>W. Ebert, A. Vescan, P. Gluche, T. Borst, and E. Kohn, *Diamond Relat. Mater.* **6**, 329 (1997).
- <sup>2</sup>P. Gluche, S.D. Wolter, T.H. Borst, W. Ebert, A. Vescan, and E. Kohn, *IEEE Electron Device Lett.* **17**, 270 (1996).
- <sup>3</sup>W. Mönch, *Europhys. Lett.* **27**, 479 (1994).
- <sup>4</sup>R. Graupner, M. Hollering, A. Ziegler, J. Ristein, L. Ley, and A. Stampfl, *Phys. Rev. B* **55**, 10 841 (1997).
- <sup>5</sup>G. Comelli, J. Stöhr, C.J. Robinson, and W. Jark, *Phys. Rev. B* **38**, 7511 (1988).
- <sup>6</sup>F.L. Coffman, R. Cao, P.A. Pianetta, S. Kapoor, M. Kelly, and L.J. Terminello, *Appl. Phys. Lett.* **69**, 568 (1996).
- <sup>7</sup>A. Gutiérrez, M.F. López, I. García, and A. Vázquez, *J. Vac. Sci. Technol. A* **15**, 294 (1997).
- <sup>8</sup>B.D. Thoms, M.S. Owens, J.E. Butler, and C. Spiro, *Appl. Phys. Lett.* **65**, 2957 (1994).
- <sup>9</sup>O.M. Küttel, L. Diederich, E. Schaller, O. Carnal, and L. Schlapbach, *Surf. Sci.* **337**, L812 (1995).
- <sup>10</sup>B.D. Thoms and J.E. Butler, *Surf. Sci.* **328**, 291 (1995).
- <sup>11</sup>R. Graupner, F. Maier, J. Ristein, L. Ley, and Ch. Jung, *Phys. Rev. B* **57**, 12 397 (1998).
- <sup>12</sup>J.B. Cui, K. Amtmann, J. Ristein, and L. Ley, *J. Appl. Phys.* **83**, 7929 (1998).
- <sup>13</sup>W. Gudat and C. Kunz, *Phys. Rev. Lett.* **29**, 169 (1972).
- <sup>14</sup>E.L. Shirley, *Phys. Rev. Lett.* **80**, 794 (1998).
- <sup>15</sup>J.F. Morar, F.J. Himpsel, G. Hollinger, G. Hughes, and J.L. Jordan, *Phys. Rev. Lett.* **54**, 1960 (1985).
- <sup>16</sup>J. Stöhr, *NEXAFS-Spectroscopy* (Springer-Verlag, Berlin, 1992).
- <sup>17</sup>F. Sette, J. Stöhr, and A.P. Hitchcock, *J. Chem. Phys.* **81**, 4906 (1984).
- <sup>18</sup>J.A. Horseley, J. Stöhr, A.P. Hitchcock, D.C. Newbury, A.L. Johnson, and F. Sette, *J. Chem. Phys.* **83**, 6099 (1985).
- <sup>19</sup>A.P. Hitchcock, D.C. Newbury, I. Ishii, J. Stöhr, J.A. Horseley, R.D. Redwing, A.L. Johnson, and F. Sette, *J. Chem. Phys.* **83**, 6099 (1985).
- <sup>20</sup>J.F. Morar, F.J. Himpsel, G. Hollinger, J.L. Jordon, G. Hughes, and F.R. McFeely, *Phys. Rev. B* **33**, 1346 (1986).
- <sup>21</sup>G. Kern, J. Hafner, and G. Kresse, *Surf. Sci.* **352-354**, 745 (1996).
- <sup>22</sup>G. Kern, J. Hafner, and G. Kresse, *Surf. Sci.* **366**, 445 (1996). In this paper, Figs. 5 and 6 have been mixed up.
- <sup>23</sup>K.A. Jackson and M.R. Pederson, *Phys. Rev. Lett.* **67**, 2521 (1991).
- <sup>24</sup>J. Nithianandam, *Phys. Rev. Lett.* **69**, 3108 (1992).
- <sup>25</sup>Y. Ma, P. Skytt, N. Wassdahl, P. Glans, D.C. Mancini, J. Guo, and J. Nordgren, *Phys. Rev. Lett.* **71**, 3725 (1993).
- <sup>26</sup>R.J. Elliott, *Phys. Rev. Lett.* **108**, 1384 (1957).
- <sup>27</sup>A. Mainwood and A.M. Stoneham, *J. Phys.: Condens. Matter* **6**, 4917 (1994).
- <sup>28</sup>F. Mauri and R. Car, *Phys. Rev. Lett.* **75**, 3166 (1995).
- <sup>29</sup>S. Tanaka and Y. Kayanuma, *Solid State Commun.* **100**, 77 (1996).
- <sup>30</sup>L. Diederich, O.M. Küttel, P. Aebi, E. Maillard-Schaller, R. Fasel, and L. Schlapbach, *Diamond Relat. Mater.* **7**, 660 (1998).
- <sup>31</sup>J. B. Cui, R. Graupner, J. Ristein, and L. Ley, *Diamond Relat. Mater.* **8**, 748 (1999).
- <sup>32</sup>J. Faul, G. Neuhold, L. Ley, J. Fraxedas, S. Zollner, J.D. Riley, and R.C.G. Leckey, *Phys. Rev. B* **50**, 7384 (1994).